Mineral Chemistry and REE Distribution in Monazite from Coastal Sediments between Bhavanapadu and Baruva, Srikakulam District, Andhra Pradesh, East Coast of India

[1]T. Sankara Rao, [2]Ch. Ravi Sekhar, [3]K.N. Murali Krishna, [4]K.S.N. Reddy
[1]Assistnat Professor, [2]Assistnat Professor, [3]Associate Professor, [4]Professor
[1]Department of Geology, M.R. (A) College, Vizianagaram, Andhra Pradesh, India
[2&4]Department of Geology, Andhra University, Visakhapatnam-530003
[3]Department of Civil Engineering, Sasi Institute of Technology & Engineering

Abstract

The mineral chemistry of monazite from coastal sediments along the Bhavanapadu–Baruva sector, Srikakulam District, Andhra Pradesh, East Coast of India, was investigated. Monazite grains in berm sediments contain average ThO_2 and UO_2 concentrations of 11.03 wt.% and 0.40 wt.%, respectively, while those in dune sediments average 11.81 wt.% ThO_2 and 0.65 wt.% UO_2. Total rare earth element (REE) contents are comparable in both environments, averaging 58.64 wt.% in beach and 57.94 wt.% in dune sediments, with La, Ce, and Nd as the dominant REEs. A consistent feature of all analyzed monazite is that total REE abundances exceed the combined concentrations of actinides (Th+U). Monazite occurring in fine-grained fractions, interpreted to have formed after garnet breakdown, shows marked enrichment in Y and heavy REEs (HREEs). Chondrite-normalized REE patterns exhibit strong enrichment in light REEs (LREEs), attributed to the preferential incorporation of lighter lanthanides during crystallization. Positive Eu anomalies further suggest that monazite crystallized from a magmatic or anatectic melt under high oxygen fugacity conditions.

Keywords. Coastal sediments, Berm, Dune, Monazite, EPMA, REE, lanthanides.

I. INTRODUCTION

Rare earth element (REE) abundances and distribution patterns are critical for tracing sediment provenance, often providing greater discrimination than major and trace element data [Mohanty et al., 2003; Panda et al., 2003]. Monazite, a LREE-rich phosphate, is a key mineral for such studies due to its chemical stability, high Th-U-REE content, and applicability to geochemical and geochronological techniques including compositional analysis [Yang et al., 2006], SHRIMP dating [Wan et al., 2007], and age mapping [Williams et al., 1999].Monazite occurs as an accessory phase in metaluminous to peraluminous granitoids and in pelitic schists and gneisses from greenschist to granulite facies. Its resistance to weathering leads to concentration in beach placers [Suzuki et al., 1994; Spear & Pyle, 2002], where it serves as an economic source of thorium and REEs. Incorporation of Th and U into the monazite lattice is facilitated by ionic radius and charge compatibility with Si and Ca [Grammaccili & Segalstad, 1978].[Overstreet][1967]In India, monazite geochemistry has been widely studied in Eastern Ghats Mobile Belt (EGMB) lithologies [Murthy, 1958; Kamineni & Rao, 1988; Rao et al., 1993; Simmat & Raith, 2008] and in coastal placers of Andhra Pradesh [Rajasekhara Reddy et al., 1998; Bangaku Naidu et al., 2016], Odisha [Singh et al., 2023], and Tamil Nadu [Natarajan et al., 2023], indicating derivation from EGMB khondalites, charnockites, and pegmatites.However, detailed mineral-chemical data for monazite from the Bhavanapadu–Baruva coast, Srikakulam District, remain unavailable. Using electron probe microanalysis (EPMA) [Williams & Jercinovic, 2002], this study characterizes detrital monazite geochemistry from this sector to constrain ThO_2, UO_2, and REE systematics, interpret source melt redox conditions, and evaluate EGMB provenance linkages.

II. STUDY AREA AND REGINAL GEOLOGY

The study covers a 44 km coastal stretch between Bhavanapadu and Baruva in Srikakulam District, Andhra Pradesh, East Coast of India. Bhavanapadu, a village and Panchayat in Santha Bommalimandal, hosts a

fishing harbour and is accessible by road from Palasa-Kasibugga. The nearest railway stations are Naupada and Palasa-Kasibugga, with bus connectivity from Sompeta. The Mahendratanaya River discharges into the Bay of Bengal at this location. Geographically, the area lies between 18°32′–18°53′ N and 84°14′–84°35′ E (Fig. 1). Survey of India toposheets 74 B/6, B/9, and B/10 were used to prepare the base map.

Beach sands in the study area are derived from sediments transported by rivers and streams draining the hinterland and adjacent landforms. The hinterland exposes a diverse suite of lithounits ranging from Archean to Quaternary age, forming part of the Eastern Ghats Granulite Belt (EGGB) on the eastern margin of the Indian Peninsular Shield. The EGGB comprises high-grade granulites and gneissic rocks. Previous geological investigations, including work by the Geological Survey of India, have established a generalized stratigraphic sequence for Srikakulam and Vizianagaram districts [Varaprasada Rao, 1963; Sharma et al., 1974; Venkata Subba et al., 1978]. The coastal zone is dominated by extensive alluvial plains.

III. MATERIALS AND METHODS

Ten surficial sediment samples five each from berm and dune environments were collected along five coast-perpendicular traverses spaced at 10 km intervals (Fig. 1). A 100 g representative split was obtained by coning and quartering. Samples were treated with 6% H_2O_2 and dilute HCl to remove organic matter and carbonate shell material, respectively, then washed, dried, and subjected to grain-size analysis. Heavy minerals were separated using bromoform (specific gravity 2.89). The heavy fractions were washed with $SnCl_2$ to eliminate Fe-Mn coatings, rinsed with distilled water, and oven-dried at 60°C. Monazite grains were identified under a binocular microscope based on optical properties. Thirty-two monazite grains from beach and dune samples were selected for electron probe microanalysis (EPMA).

Monazite chemical analyses were performed using a CAMECA SX-100 electron probe microanalyzer (EPMA) equipped with four wavelength-dispersive spectrometers (WDS) at the Indian School of Mines, Dhanbad. Prior to EPMA, monazite grains were identified by optical microscopy and scanning electron microscopy with energy-dispersive X-ray spectroscopy (SEM-EDS) for compositional verification. Selected grains were prepared as polished thin sections and coated with a 20 nm carbon film.EPMA operating conditions were 20 kV accelerating voltage, 200–400 nA beam current, and ~2 µm beam diameter using a LaB_6 source. Quantitative analyses and U–Th–Pb chemical dating were carried out using the CAMECA PeakSight software. Pb, Th, and U were measured simultaneously on LPET and PET crystals in 'Peak Background–Peak Background' mode with 10 counting cycles. Pb-Mβ was used instead of Pb-Mα to avoid overlap with Y-Lγ lines, and exponential background fitting was applied to improve precision [Jercinovic & Williams, 2005; Williams et al., 2006]. U-Mβ was measured to avoid Th-Mβ interference [Suzuki & Kato, 2008].Calibration used both natural and synthetic standards: vanadinite (Pb), UO_2 (U), ThO_2 (Th), REE-bearing glass (REEs), apatite (P), YAG (Y), hematite (Fe), corundum (Al), and Th-glass (Si). Major spectral interferences, including U-Mζ$_2$ and Pr-Lη on Pb-Mβ, and Th-M_3N_4 on U-Mβ, were corrected offline. Analytical protocols followed established procedures [Nasdala et al., 2006; Pant et al., 2009; Bhowmik et al., 2010; Bhandari et al., 2011; Ruschel et al., 2012; Pandey et al., 2019]. Analytical precision for Pb in monazite is typically limited to ~2% due to spectrometer variations and instrumental drift [Spear et al., 2009].

IV. RESULTS AND DISCUSSION

Chemical compositions of monazite from berm (n=16) and dune (n=16) sediments, determined by EPMA, are summarized in Tables 1 and 2. Berm monazites are Ce-monazite with the following ranges (wt%): ThO_2 6.23–15.20 (avg. 11.03), UO_2 0.17–0.81, PbO 0.16–0.73, P_2O_5 26.00–29.11, Y_2O_3 0.04–1.14, La_2O_3 10.26–15.60, Ce_2O_3 25.03–30.47, Pr_2O_3 2.78–3.94, Nd_2O_3 7.94–12.49, Sm_2O_3 0.93–1.80, Eu_2O_3 0.15–0.75, Gd_2O_3 0.28–0.97, Tb_2O_3 0.01–0.09, Dy_2O_3 0.06–0.19, Ho_2O_3 0.04–0.28, Tm_2O_3 0.09–0.21, SiO_2 0.32–2.91, and CaO 0.42–1.70. Dune monazites show similar Ce-monazite compositions (wt%): ThO_2 7.00–16.10, UO_2 0.26–2.07, PbO 0.24–0.69, P_2O_5 24.98–29.04, Y_2O_3 0.08–1.79, La_2O_3 10.26–14.28, Ce_2O_3 25.12–31.91, Pr_2O_3 2.81–3.59, Nd_2O_3 7.89–11.31, Sm_2O_3 0.95–1.84, Eu_2O_3 0.00–0.75, Gd_2O_3 0.31–1.50, Tb_2O_3 0.00–0.15, Dy_2O_3 0.06–0.21, Ho_2O_3 0.03–0.49, Tm_2O_3 0.09–0.19, SiO_2 0.30–2.58, and CaO 0.39–1.46.Significant grain-to-grain compositional variability is observed in both settings, consistent with derivation from heterogeneous source lithologies (Tables 3, 4).Monazite typically contains 4-12% ThO_2, while cheralite, a variety of monazite, can have up to 30% ThO_2 due to substitution of La by Th and Ce by Ca (Bowie and Horne, 1953).

In the study area, monazites are enriched in ThO_2, ranging from: 6.23% to 15.57% in berm sediments and 7.00% to 16.50% in dune sediments

Approximately 56% of the analyzed monazite grains contain >12 wt% ThO_2, classifying them as cheralite, whereas the remaining 44% have <12 wt% ThO_2. The occurrence of cheralite-rich monazite has previously been documented in nearby coastal sectors, including Kalingapatnam–Baruva [Rajasekhara Reddy & Siva Sankar Prasad, 1997] and Visakhapatnam–Bhimunipatnam [Rao & Prakasa Rao, 1980]. Within the Eastern Ghats Granulite Belt (EGGB), monazite ThO_2 contents vary with lithology. Khondalites typically exhibit relatively uniform thorium concentrations of 6–10 wt% ThO_2 [Murthy & Divakara Rao, 1999; Kamineni et al., 1991], whereas charnockites display greater variability, with ThO_2 ranging from 9–10 wt% [Mallikharjuna Rao et al., 1999; Kamineni et al., 1991].

The mineral assemblage of the study area shows strong affinity to the Eastern Ghats Group, especially the Khondalite suite. This suite is characterized by major phases including garnet, biotite, sillimanite, cordierite, K-feldspar, plagioclase, and quartz, with accessory magnetite, ilmenite, rutile, sphene, apatite, and monazite [Murthy & Divakara Rao, 1999]. The Charnockite suite, comprising charnockite and enderbite, contains orthopyroxene, clinopyroxene, garnet, biotite, magnetite, ilmenite, monazite, K-feldspar, plagioclase, and quartz [Mallikharjuna Rao et al., 1999]. Monazite occurrence differs between lithologies: in charnockites it forms relatively coarse grains of 200–2000 µm, whereas in khondalites it occurs as fine inclusions of ~50 µm within garnet and cordierite [Kamineni et al., 1991].

4.1 Rare Earth Elements (REE)

REE concentrations and chondrite-normalized patterns are effective indicators of sediment provenance and often provide greater discrimination than major or trace element data alone. The EPMA-derived monazite compositions from the study area are given in Tables 3 and 4. For provenance interpretation, REE abundances were normalized to chondrite values [Taylor & Mc Lennan, 1985], with emphasis on the behavior of light REE (LREE) versus heavy REE (HREE).During magmatic crystallization, REEs have large ionic radii (La: 1.06 Å to Lu: 0.85 Å) and high ionic charges, which limit their substitution for major cations due to their low abundances. Among REEs, Y and HREE possess smaller ionic radii relative to LREE, resulting in reduced compatibility with the monazite structure.[Felsche, 1976]

The chondrite-normalized REE pattern of monazites from the study area shows strong LREE enrichment with Ce > La > Nd > Pr > Sm > Gd. This pattern is comparable to monazites reported from the Eastern Ghats Granulite Belt (EGGB) and Kalingapatnam–Baruva coastal sands [Rajasekhara Reddy & Siva Sankar Prasad, 1997]. Monazites are characterized by higher LREE relative to HREE and low Y concentrations. This LREE-enriched signature is typical of garnet-bearing assemblages, where monazite preferentially excludes Y and HREE due to crystal-chemical constraints [Mason & Moore, 1982; Kamineni et al., 1991].

Monazite grains from the study area are strongly enriched in LREE relative to HREE and display a pronounced Eu anomaly. This fractionated REE signature is clearly expressed in ternary diagrams, which highlight LREE dominance in monazite compositions.Total REE (ΣREE) contents in berm monazites range from 51.95–62.88 wt% (avg. 58.64 wt%), while dune monazites range from 53.05–63.21 wt% (avg. 57.94 wt%). In both settings, LREE overwhelmingly dominate over HREE.The ΣLREE/(Th+U) ratio, which reflects the substitution of LREE by Th and U in the monazite lattice, varies from 3.19–9.74 (avg. 5.35) in berm sediments and 2.71–8.33 (avg. 4.96) in dune sediments. These values indicate that Th and U substitute for REE in the crystal structure, consistent with Kamineni et al.. Variation in this ratio likely reflects differences in geochemical conditions during monazite crystallization or subsequent alteration.[1991]Overall, monazite REE chemistry provides key constraints on provenance. The strong LREE enrichment, Ce dominance, and Eu anomaly are characteristic of the study area. The ΣLREE/(Th+U) ratio further documents Th–U–REE coupled substitution [Kamineni et al., 1991].Coastal monazites show elevated LREE, depleted HREE, and low Y contents, consistent with derivation from metapelitic khondalite and charnockite sources of the EGGB. The association with garnet supports this interpretation. Chondrite-normalized REE patterns (Figs. 3a, b) are broadly uniform and display a positive Eu anomaly in most grains,

with negative Eu anomalies in a few berm grains (nos. 4, 10, 16), indicating a largely consistent source with minor heterogeneity.

4.2 Eu Anomaly

The europium anomaly, expressed as Eu/Eu_, provides insight into redox conditions during monazite crystallization. Eu/Eu_ >1 indicates a positive anomaly, whereas values <1 reflect a negative anomaly. Studied monazites yield average Eu/Eu_ of 1.35 in berm sediments and 1.23 in dune sediments, indicating positive Eu anomalies (Tables 3, 4).As noted by Henderson and Pankhurst, Eu anomalies arise from enrichment or depletion of Eu relative to neighboring REE during magmatic differentiation, controlled by plagioclase fractionation and oxygen fugacity. REE patterns in monazite are further modulated by the evolving mineral assemblage and source-rock composition [Zhu & O'Nions, 1999].[1984]The occurrence of magnetite in Khondalite and Charnockite suites of the EGGB implies relatively oxidizing conditions during crystallization. Under high fO_2, Eu occurs as Eu^{3+}, which is incompatible with the plagioclase structure and becomes enriched in the melt. Conversely, under reducing conditions, Eu^{2+} can substitute for Ca^{2+} in plagioclase, leading to Eu depletion in the residual melt. Thus, the valence state of Eu directly controls the magnitude and sign of the Eu anomaly.The observed enrichment of Eu^{3+} relative to other REE produces the positive Eu anomalies in chondrite-normalized patterns of the studied monazites. In charnockites and enderbites from the Visakhapatnam region, the coexistence of magnetite and positive Eu anomalies is consistent with high oxygen fugacity during magma genesis, typical of oxidized calc-alkaline magmas [Mallikharjuna Rao et al., 1999].

4.3 ΣLLn/HLn Ratios

Chondrite-normalized (ΣLREE/HREE)cn ratios confirm strong LREE enrichment over HREE in the studied monazites, ranging from 11.17–26.50 in berm sediments and 7.60–26.69 in dune sediments. Such high ratios indicate preferential partitioning of LREE into monazite during partial melting and crystallization [Henderson & Pankhurst, 1984].The (La/Sm)cn ratio further constrains LREE fractionation, varying from 7.25–18.55 (avg. 14.06) in berm monazites and 7.56–17.78 (avg. 11.45) in dune monazites (Tables 3, 4). These values reflect significant fractionation within the LREE group during magmatic evolution.

4.4 Nd/Ce and La/Ce Ratios

Nd/Ce ratios in the studied monazites range from 0.31–0.46 (avg. 0.35) in berm sediments and 0.29–0.41 (avg. 0.36) in dune sediments. La/Ce ratios vary from 0.38–0.54 (avg. 0.46) in both settings. These values are comparable to monazites from the Kalingapatnam–Baruva coast, Andhra Pradesh [Rajasekhara Reddy & Siva Sankar Prasad, 1997], khondalites [Kamineni & Rao, 1988] and charnockites [Kamineni et al., 1991] of the Eastern Ghats Granulite Belt, India, and to monazites from Eastern Minas Gerais, Brazil [Murata et al., 1958].

4.5 Zoning in Monazite

Monazite commonly displays compositional zoning, with concentric, patchy, and intergrowth textures recognized as the three principal types [Zhu & O'Nions, 1999]. Zoning has been widely used to evaluate intra-grain chemical heterogeneity and growth history [Williams et al., 1999; Zhu & O'Nions, 1999]. In the study area, Th content varies significantly among grains, reflecting inheritance from compositionally diverse crystalline source rocks. Complex patchy zoning indicates substantial chemical and temporal modification driven by deformation and fluid infiltration during prograde to retrograde metamorphic events. While some grains preserve chemical zoning, others are homogeneous or well-rounded, suggesting extensive mechanical abrasion during transport. Zoned domains in monazites are depleted in La, Pr, Nd, Sm, and Eu relative to unzoned domains, indicating preferential fractionation of LREE during recrystallization or alteration.

V Conclusions

1. ThO_2 in monazites ranges 6.23–15.57 wt% (avg. 11.03 wt%) in berm and 7.00–16.50 wt% (avg. 11.81 wt%) in dune sediments. With 56% of grains >12 wt% ThO_2, they classify as cheralite.

2. Monazite compositions show ΣREE > (U+Th) with LREE >> HREE, consistent with derivation from garnet-bearing khondalites and charnockites of the EGGB, where HREE and Y partition into coexisting garnet.
3. Positive Eu anomalies (avg. Eu/Eu_ = 1.35 berm, 1.23 dune) indicate crystallization under high fO_2, typical of oxidized calc-alkaline melts.
4. High (ΣLREE/HREE)cn and (La/Sm)cn ratios document extensive LREE fractionation during partial melting and crystallization.
5. Nd/Ce and La/Ce ratios match EGGB khondalites, charnockites, and Kalingapatnam–Baruva placers, supporting local provenance.
6. Patchy zoning and LREE depletion in zoned domains record fluid-mediated recrystallization during metamorphism; rounded, unzoned grains reflect mechanical weathering.

Acknowledgement

The first author gratefully acknowledges the Head, Department of Geology, Andhra University, Visakhapatnam, for providing laboratory facilities and for continued support and encouragement during this work. Sincere thanks are also extended to the Geological Survey of India (GSI), Hyderabad, for access to EPMA facilities used for mineral-chemical analyses. The Principal, M.R.(A) College, is thanked for constant encouragement.

References

[1] Aftalion, M., Bowes, D.R., Dash, B. and Dempster, T.J., 1988. Late Proterozoic charnockites in Orissa, India: A U-Pb and Rb - Sr isotopic study. Jour. Geol., 96: 663-676.

[2] Bangaku Naidu, K., Reddy, K.S.N., Ravi Sekhar, Ch., Ganapathi Rao, P. and Murali Krishna, K.N., 2016. REE geochemistry of monazites from coastal sands between Bhimunipatnam and Konada, Andhra Pradesh, East coast of India. Curr. Sci., 110(8): 1550-1559.

[3] Divakara Rao, V. and Murthy, N.N., 1998a. Evolution of the Eastern Ghats Granulite Belt, India. Gondwana Research Group Memoir No. 4:1-18.

[4] Divakara Rao, V., 1984. Khondalites from the Eastern Ghats granulite belt, geochemistry and origin. Geophy. Res. Bull., 21(3): 233-242.

[5] Felsche, J., 1976. Yttrium and lanthanides, section A. In K. H. Wedepohl, Ed., Handbook of Geochemistry, v. II, section 39, 57-71p.

[6] Grammaccioli, C.M. and Segalstad, T.V., 1978. A uranium and thorium-rich monazite from a south-alpine pegmatite at Piona, Italy. Am. Mineral. 63: 757-761.

[7] Henderson, P. and Pankhrust, R.J., 1984. Development in Geochemistry, Rare Earth Element geochemistry, Elsevier, Amsterdam, 510.

[8] Iizuka, T., McCulloch, M.T., Komiya, T., Shibuya, T., Ohta, K., Ozawa, H., Sugimura, E. and Collerson, K.D., 2010. Monazite geochronology and geochemistry of meta-sediments in the Narryer Gneiss complex, Western Australia: constraints on the tectonothermal history and provenance. Contrib Mineral Petrol, 160: 803-823.

[9] Kamineni, D.C., and Rao, A.T., 1988. Sapphirine granulites from the Kakanuru area, Eastern Ghats, India. American Mineralogist, 73: 692-700.

[10] Kamineni, D.C., Rao, A.T. and Bonardi, M., 1991. The geochemistry of monazite types from the Eastern Ghats Granulite Terrain, India. Mineralogy and Petrology, 45: 119-130.

[11] Kshira Sagar, T.V.S.R. and Nagamalleswara Rao, B., 1993. Indian Mining Engi. Jour., XLI: 31-33.

[12] Kusiak, M.A., Alvarez, I.G., Kerrich, R. and Konecny, P., 2014. REE mobilization and low temperature monazite in basinal brine environments. Planet Formation, Crustal Growth, and the Evolving Lithosphere, 83-85.

[13] Mallikharjuna Rao, J., Divakara Rao, V. and Murthy, N.N., 1999. Charnockite from EGMB - Geochemistry, protolith character and tectonic relevance. In: Memoir: 5, A.T. Rao, Divakara Rao, V. and Yoshida. M., (Eds), Gondwana Research Group: 31-50.

[14] Mohanty, A.K., Das, S.K., Vijayan, V., Sengupta, D., and Saha, S.K., 2003. Geochemical studies of monazite sands of Chhatrapur beach placer deposit of Orissa, India by PIXE and EDXRF method. Nucl. Instr. Meth. Phy. Res. B 211: 145-154.

[15] Murata, K.J., Dutra, C.V., Teixeira da Costa, M. and Branco, J.J.R., 1958. Composition of monazites from pegmatites in Eastern Minas Gerais, Brasil. Geochim. Cosmochim. Acta, 16: 1-14.

[16] Murthy, M.S., 1958. Occurrence of monazite in the charnockites of Visakhapatnam. Curr.Sci., 27: 347-348.

[17] Murthy, N.N. and Divakara Rao, V., 1999. Geochemistry, Provenance and depositional environment of the khondalites from the Eastern Ghats Mobile Belt. In: Rao, A.T, Divakara Rao. V and Yoshida. M (Eds.) Eastern Ghats Granulites, Memoir No: 5: 15 – 30.

[18] Narayana, B.L., Rama Rao, P., Reddy, G.L.N. and Divakara Rao, V., 1995. Geochemistry and origin of megacrystic charnockites and granites from Eastern Ghat Granulite Belt. Proceedings of symposium on India and Antarctica during the Precambrian and granulite and crustal processes in East Gondwana. Dec. 1-3, Andhra University, Visakhapatnam, Abstract: 36-37.

[19] Natarajan, T., Sahoo, S. K., Nakajima, T., Veerasamy, N., Yamazaki, S., Inoue, K. andRamola, R. C. (2023). Distribution of 226Ra, 232Th and 40K in Kanyakumari beach placer deposits along Tamil Nadu coast, India. Journal of Radioanalytical and Nuclear Chemistry, 1-9.

[20] Overstreet, W. C., 1967. The geologic occurrence of monazite, U. S. Geological Professional Paper 530, 327.

[21] Panda, N.K., Rajagopalan, V. and Ravi, G.S., 2003. Rare earth element geochemistry of placer monazites from Kalingapatnam coast, Srikakulam district, Andhra Pradesh. Jour. Geol. Soc. India, 62: 429-438.

[22] Rajasekhara Reddy, D. and Siva Sankara Prasad, V., 1997. Thorium - rich monazites from the beach sands of Kalingapatnam-Baruva coast, Andhra Pradesh, East coast of India. Curr. Sci., 73(10): 880-882.

[23] Rajasekhara Reddy, D., Malathi, V., Reddy, K.S.N. and Deva Varma, D., 1998. Heavy minerals in different environments of beaches between Pudimadaka and Pentakota, East coast of India. Jour. Ind. Acad. Geol. Sci., 41(2): 47-54.

[24] Rao, A.T. and Prakasa Rao, Ch.S., 1980. Cheralite from beach placers of Visakhapatnam-Bhimunipatnam coast. Ind. Jour. Mar. Sci., 9: 214-216.

[25] Rao, A.T., Fonarev, V.I., Konilov, A.N. and Romanenko, M., 1998. Electron Microprobe dating of monazite from Spinel granulite in the Eastern Ghats belt, India. Jour. Geol. Soc. Ind., 52: 345-350.

[26] Rao, A.T., Rao, J.U. and Yoshida, M., 1993. Geochemistry and tectonic evolution of the pyroxene granulites from Visakhapatnam area in the Eastern Ghats Granulite Belt, India. Jour. Geosci., Osaka City University, 36: 135 – 150.

[27] Simmat, R. and Raith, M.M., 2008. U-Th-Pb monazite geochronometry of the Eastern Ghats Belt, India: Timing and spatial disposition of poly-metamorphism. Precambrian Research, 162: 16-39.

[28] Singh, D., Basu, S., Mishra, B., Prusty, S., Kundu, T. and Rao, R. (2023).Textural and Chemical Characters of Lean Grade Placer Monazite of Bramhagiri coast, Odisha, India. Minerals, 13(6), 742.

[29] Spear F. S. and Pyle J. M. 2002. Phosphates in metamorphic rocks. Rev. Mineral. 48: 293–335

[30] Suzuki, K., Adachi, M., and Kajizuka, I., 1994. Electron microprobe observations of Pb diffusion in metamorphosed detrital monazites. Earth Planet. Sci. Lett. 128: 391– 405.

[31] Wan, Y., Song, T., Liu, D., Yang, T., Yin, X., Chen, Z. and Zhang, Q., 2007. Mesozoic monazite in Neoproterozoic metasediments: Evidence for lowgrade metamorphism of Sinian sediments during Triassic continental collision, Liaodong Peninsula, NE China. Geochem. Jour., 41: 47-55.

[32] Williams M.L, Jercinovic M.J. and Terry M.P., 1999. Age mapping and dating of monazite on the electron microprobe; deconvoluting multistage tectonic histories. Geol., 27:1023 - 1026.

[33] Williams, M.L and Jercinovic, M.J., 2002. Microprobe monazite geochronology putting absolute time into microstructural analysis. Jour. Struc. Geol. 24: 1013–1028.

[34] Yang, S., Li, C. and Yokoyama, K., 2006. Elemental compositions and monazite age patterns of core sediments in the Changjiang Delta: Implications for sediment provenance and development history of the Changjiang River. Earth and Planetary Science Letters, 245:762-776.

[35] Zhu, X.K. and O'Nions, R.K., 1999. Zonation of monazite in metamorphic rocks and its implications for high temperature thermochronology: a case study from the Lewisian terrain. Earth and Planetary Science Letters 171: 209–220.

Table 1 Chemical composition of monazites from berm environment between Bhavanapadu and Baruva

Sample No.	1B			2B			3B			4B			5B			
Grain No.	1	2	3	4	5	6	7	8	9	10	11	12	13	14	15	16
SiO_2	1.47	0.39	0.75	2.91	0.80	0.32	1.05	1.61	1.41	1.38	1.31	1.24	1.08	1.61	1.06	0.47
CaO	1.15	1.03	1.70	1.11	0.83	1.11	1.09	0.81	1.13	1.13	0.42	1.67	1.42	1.02	1.38	0.80
UO_2	0.27	0.66	0.81	0.49	0.24	0.61	0.24	0.25	0.43	0.30	0.28	0.56	0.27	0.33	0.56	0.17
ThO_2	11.33	9.70	10.32	15.20	8.09	8.00	10.62	12.35	10.61	13.20	10.35	14.57	12.72	11.07	12.05	6.23
PbO	0.43	0.28	0.46	0.73	0.26	0.31	0.35	0.38	0.42	0.46	0.32	0.31	0.40	0.45	0.26	0.16
P_2O_5	27.84	28.67	27.65	27.08	27.94	28.55	27.09	27.17	27.56	26.15	26.00	27.00	27.02	27.00	27.62	29.11
Y_2O_3	0.20	0.14	0.30	0.18	0.08	0.13	0.08	0.15	0.21	0.17	0.09	1.14	0.04	0.22	0.09	0.12
La_2O_3	13.16	11.68	13.12	10.26	14.69	14.16	13.95	11.86	13.05	13.35	14.26	14.05	12.46	13.25	13.21	15.60
Ce_2O_3	28.02	25.19	27.49	25.03	30.47	29.75	30.13	29.83	28.81	28.89	29.98	25.40	28.61	29.07	29.05	31.37
Pr_2O_3	3.26	3.78	3.15	3.22	3.37	3.29	3.35	3.29	3.32	3.23	3.72	2.81	3.44	3.31	3.31	3.37
Nd_2O_3	9.97	12.49	9.51	10.22	10.25	10.13	10.02	9.58	9.85	9.14	10.21	7.94	10.55	9.87	8.63	9.95
SmO	1.06	1.80	1.54	1.59	1.08	1.57	0.94	0.93	1.15	1.12	1.26	1.23	1.07	1.02	1.21	1.15
EuO	0.45	0.51	0.61	0.75	0.62	0.67	0.52	0.45	0.39	0.15	0.53	0.45	0.32	0.33	0.61	0.45
Gd_2O_3	0.52	0.63	0.97	0.69	0.50	0.82	0.28	0.36	0.52	0.47	0.34	0.97	0.34	0.48	0.42	0.46
Tb_2O_3	0.02	0.02	0.07	0.02	0.06	0.05	0.01	0.04	0.03	0.02	0.02	0.09	0.01	0.02	0.05	0.04
Dy_2O_3	0.09	0.19	0.16	0.14	0.06	0.11	0.08	0.09	0.11	0.13	0.12	0.12	0.09	0.11	0.08	0.15
Ho_2O_3	0.14	0.19	0.28	0.21	0.11	0.27	0.04	0.08	0.12	0.08	0.07	0.28	0.04	0.10	0.09	0.12
Er_2O_3	0.00	0.00	0.00	0.00	0.00	0.00	0.00	0.00	0.00	0.00	0.00	0.00	0.00	0.00	0.00	0.00
Tm_2O_3	0.13	0.21	0.16	0.12	0.09	0.15	0.11	0.10	0.12	0.11	0.14	0.12	0.12	0.12	0.15	0.10
Yb_2O_3	0.00	0.00	0.00	0.00	0.00	0.00	0.00	0.00	0.00	0.01	0.00	0.00	0.00	0.00	0.00	0.00
Lu_2O_3	0.00	0.00	0.00	0.00	0.00	0.00	0.01	0.00	0.00	0.00	0.00	0.01	0.00	0.01	0.00	0.00
Total	99.51	97.56	99.05	99.95	99.54	100.00	99.96	99.33	99.24	99.49	99.42	99.96	100.00	99.39	99.83	99.82
Formulae normalized to 4 oxygens																
Si	0.06	0.02	0.03	0.12	0.03	0.01	0.04	0.06	0.06	0.06	0.05	0.05	0.04	0.06	0.04	0.02
Ca	0.05	0.04	0.07	0.05	0.04	0.05	0.05	0.03	0.05	0.05	0.02	0.07	0.06	0.04	0.06	0.03
U	0.00	0.01	0.01	0.00	0.00	0.01	0.00	0.00	0.00	0.00	0.00	0.01	0.00	0.00	0.00	0.00
Th	0.12	0.07	0.11	0.14	0.07	0.06	0.10	0.11	0.11	0.13	0.08	0.14	0.12	0.12	0.11	0.06
Pb	0.00	0.00	0.00	0.01	0.00	0.00	0.00	0.00	0.00	0.01	0.00	0.00	0.00	0.00	0.00	0.00
P	0.93	0.97	0.94	0.90	0.97	0.97	0.94	0.92	0.93	0.91	0.94	0.92	0.95	0.92	0.94	0.99
Y	0.00	0.00	0.01	0.00	0.00	0.00	0.00	0.00	0.00	0.00	0.00	0.02	0.00	0.00	0.00	0.00
La	0.19	0.17	0.20	0.14	0.21	0.22	0.21	0.21	0.19	0.20	0.19	0.21	0.18	0.20	0.19	0.23
Ce	0.42	0.43	0.41	0.39	0.44	0.44	0.44	0.44	0.42	0.44	0.43	0.38	0.42	0.43	0.42	0.45
Pr	0.05	0.06	0.05	0.05	0.05	0.05	0.05	0.05	0.05	0.05	0.05	0.04	0.05	0.05	0.05	0.05
Nd	0.14	0.18	0.14	0.16	0.14	0.15	0.14	0.14	0.14	0.14	0.16	0.11	0.15	0.14	0.14	0.14
Sm	0.01	0.02	0.02	0.02	0.01	0.02	0.01	0.01	0.02	0.02	0.02	0.02	0.01	0.01	0.02	0.02
Ho	0.00	0.00	0.00	0.00	0.00	0.00	0.00	0.00	0.00	0.00	0.00	0.00	0.00	0.00	0.00	0.00
Er	0.00	0.00	0.00	0.00	0.00	0.00	0.00	0.00	0.00	0.00	0.00	0.00	0.00	0.00	0.00	0.00
Tm	0.00	0.00	0.00	0.00	0.00	0.00	0.00	0.00	0.00	0.00	0.00	0.00	0.00	0.00	0.00	0.00
Yb	0.00	0.00	0.00	0.00	0.00	0.00	0.00	0.00	0.00	0.00	0.00	0.00	0.00	0.00	0.00	0.00
Lu	0.00	0.00	0.00	0.00	0.00	0.00	0.00	0.00	0.00	0.00	0.00	0.00	0.00	0.00	0.00	0.00
Total	2.00	2.01	2.01	2.00	2.00	2.01	2.01	2.00	2.00	2.02	2.00	2.01	2.00	2.01	2.01	1.99

Table 2 Chemical composition of monazites from dune sediments between Bhavanapadu and Baruva

Sample No.	1D			2D				3D			4D			5D		
Grain No.	1	2	3	4	5	6	7	8	9	10	11	12	13	14	15	16
SiO_2	2.42	1.11	0.30	1.53	0.44	1.41	2.07	0.39	2.57	1.01	1.52	1.97	0.87	0.53	0.60	2.58
CaO	0.82	0.42	1.16	1.23	1.16	1.44	1.31	1.46	0.39	1.41	1.15	0.74	1.16	1.12	1.40	0.55
UO_2	2.07	0.33	0.32	0.57	0.40	0.49	0.34	0.47	0.31	0.32	0.50	1.53	0.26	0.55	0.34	1.60

ThO_2	14.91	7.99	7.00	13.25	8.27	14.47	16.10	10.18	14.06	12.54	13.32	12.21	9.52	9.40	10.36	15.33
PbO	0.69	0.24	0.25	0.46	0.33	0.54	0.56	0.60	0.33	0.40	0.38	0.50	0.32	0.31	0.30	0.57
P_2O_5	24.98	25.65	29.04	26.00	28.10	26.26	26.56	28.63	27.19	27.80	26.51	26.05	28.38	27.75	28.05	25.22
Y_2O_3	1.07	0.08	0.33	0.20	0.36	0.32	0.11	0.11	0.48	1.46	1.09	1.79	0.08	0.26	0.92	0.45
La_2O_3	10.26	14.28	13.85	12.29	13.00	12.05	11.28	13.18	10.84	11.60	11.01	12.60	13.53	14.14	12.50	14.20
Ce_2O_3	25.12	31.91	29.98	27.16	29.42	27.12	25.79	27.80	28.13	26.24	26.46	26.23	28.99	28.72	27.51	25.26
Pr_2O_3	3.01	3.59	3.33	3.22	3.45	3.17	3.17	3.06	3.40	3.19	3.29	2.94	3.45	3.37	3.31	2.81
Nd_2O_3	9.39	10.83	10.58	10.40	10.79	9.79	10.41	11.31	8.60	9.30	10.07	7.89	10.30	10.25	10.53	8.05
SmO	1.69	1.16	1.02	1.76	1.84	1.21	1.11	1.30	1.47	1.73	1.65	1.58	0.95	1.58	1.69	1.23
EuO	0.56	0.59	0.75	0.52	0.49	0.49	0.47	0.59	0.71	0.59	0.53	0.59	0.52	0.00	0.56	0.57
Gd_2O_3	1.32	0.44	0.85	0.91	1.12	0.57	0.41	0.47	0.86	1.24	1.20	1.50	0.31	1.07	1.07	0.90
Tb_2O_3	0.12	0.05	0.06	0.07	0.08	0.03	0.01	0.00	0.04	0.13	0.12	0.15	0.03	0.06	0.09	0.08
Dy_2O_3	0.18	0.13	0.17	0.21	0.18	0.14	0.08	0.13	0.13	0.16	0.17	0.16	0.06	0.15	0.14	0.13
Ho_2O_3	0.42	0.06	0.24	0.26	0.36	0.14	0.08	0.09	0.22	0.42	0.41	0.49	0.03	0.29	0.37	0.29
Er_2O_3	0.00	0.00	0.00	0.00	0.00	0.00	0.00	0.00	0.00	0.00	0.00	0.00	0.00	0.00	0.00	0.00
Tm_2O_3	0.16	0.09	0.19	0.13	0.15	0.13	0.13	0.17	0.17	0.18	0.16	0.14	0.12	0.17	0.18	0.14
Yb_2O_3	0.01	0.00	0.00	0.00	0.00	0.00	0.00	0.00	0.00	0.00	0.00	0.00	0.02	0.00	0.00	0.00
Lu_2O_3	0.02	0.00	0.00	0.00	0.00	0.00	0.00	0.00	0.00	0.02	0.00	0.01	0.00	0.00	0.01	0.01
Total	99.22	98.95	99.42	100	99.94	99.77	99.99	99.94	99.90	99.74	99.54	99.07	98.9	99.72	99.93	99.97
Formulae normalized to 4 oxygens																
Si	0.10	0.04	0.01	0.06	0.02	0.06	0.08	0.02	0.10	0.04	0.06	0.08	0.03	0.02	0.02	0.11
Ca	0.04	0.02	0.05	0.05	0.05	0.06	0.06	0.06	0.02	0.06	0.05	0.03	0.05	0.05	0.06	0.02
U	0.02	0.00	0.00	0.01	0.00	0.00	0.00	0.00	0.00	0.00	0.00	0.01	0.00	0.00	0.00	0.01
Th	0.16	0.07	0.06	0.12	0.08	0.14	0.16	0.08	0.13	0.11	0.12	0.12	0.10	0.08	0.09	0.14
Pb	0.01	0.00	0.00	0.01	0.00	0.01	0.01	0.01	0.00	0.00	0.00	0.01	0.00	0.00	0.00	0.01
P	0.88	0.95	0.98	0.92	0.97	0.91	0.91	0.98	0.90	0.95	0.91	0.90	0.95	0.96	0.95	0.86
Y	0.02	0.00	0.01	0.00	0.01	0.01	0.00	0.00	0.01	0.03	0.03	0.04	0.00	0.01	0.03	0.01
La	0.16	0.21	0.20	0.18	0.19	0.18	0.17	0.19	0.18	0.17	0.17	0.19	0.21	0.21	0.19	0.22
Ce	0.38	0.46	0.43	0.41	0.43	0.40	0.38	0.41	0.42	0.39	0.39	0.39	0.43	0.43	0.41	0.40
Pr	0.05	0.05	0.05	0.05	0.05	0.06	0.05	0.05	0.05	0.05	0.05	0.04	0.06	0.05	0.05	0.04
Nd	0.14	0.15	0.15	0.15	0.15	0.14	0.15	0.16	0.13	0.13	0.16	0.13	0.15	0.15	0.15	0.12
Sm	0.02	0.02	0.02	0.02	0.03	0.02	0.02	0.02	0.02	0.02	0.02	0.02	0.01	0.02	0.02	0.03
Eu	0.01	0.01	0.01	0.01	0.01	0.01	0.01	0.01	0.01	0.01	0.01	0.01	0.01	0.00	0.01	0.01
Gd	0.02	0.01	0.01	0.01	0.01	0.01	0.01	0.01	0.01	0.02	0.02	0.02	0.00	0.01	0.01	0.01
Ho	0.01	0.00	0.00	0.00	0.00	0.00	0.00	0.00	0.00	0.01	0.01	0.01	0.00	0.00	0.00	0.00
Er	0.00	0.00	0.00	0.00	0.00	0.00	0.00	0.00	0.00	0.00	0.00	0.00	0.00	0.00	0.00	0.00
Tm	0.00	0.00	0.00	0.00	0.00	0.00	0.00	0.00	0.00	0.00	0.00	0.00	0.00	0.00	0.00	0.00
Yb	0.00	0.00	0.00	0.00	0.00	0.00	0.00	0.00	0.00	0.00	0.00	0.00	0.00	0.00	0.00	0.00
Lu	0.00	0.00	0.00	0.00	0.00	0.00	0.00	0.00	0.00	0.00	0.00	0.00	0.00	0.00	0.00	0.00
Total	2.0	2.0	2.0	2.0	2.0	2.0	2.0	2.0	2.0	2.0	2.0	2.0	2.0	2.0	2.0	2.0

Table 3 REE distribution in monazites from berm environment between Bhavanapadu and Baruva

Grain No.	∑REE	∑LREE	∑HREE	Th+U (Actinoides)	Th/U	∑LREE/Th+U	∑LREE/HREE	Nd/Ce	La/Ce	Th+ si	Th+ Ca	REE +Y	(∑LLn/HLn)cn	(La/Sm)cn	Eu/Eu*
1	60.76	60.31	0.45	10.63	32.39	8.37	135.24	0.37	0.42	10.68	10.77	60.85	20.35354	12.99581	1.65
2	56.07	54.31	1.75	15.13	28.8	4.31	30.29	0.31	0.55	16.78	16.24	57.21	11.1696	14.21	0.90
3	57.08	56.78	0.31	12.99	46.11	4.37	189.27	0.36	0.44	13.8	14.14	57.12	24.20	14.63	1.13

4	57.9	57.33	0.57	13.4	38.61	4.28	100.58	0.34	0.46	14.68	14.09	58.12	21.63	15.17	1.05
5	57.9	58.44	0.46	12.61	21.52	4.56	125.87	0.33	0.45	13.11	13.43	57.99	17.24	13.59	1.84
6	61.1	60.39	0.71	7.50	11.3	8.19	86.46	0.34	0.51	7.19	8.00	62.23	13.82	13.02	1.33
7	60.52	58.19	0.33	11.86	44.25	5.45	179.36	0.33	0.46	11.67	11.71	58.6	26.5	18.47	2.12
8	58.76	58.3	0.46	12.6	49.4	5.63	126.74	0.32	0.46	13.96	13.16	58.91	23.33	18.55	1.70
9	57.68	57.09	0.57	12.04	29.33	4.38	96.76	0.34	0.46	14.04	13.74	58.89	19.12	14.12	1.12
10	57.47	57.95	0.54	13.9	45.33	4.10	108.52	0.34	0.46	14.98	14.73	57.64	22.34	14.84	0.48
11	57.56	56.98	0.58	13.6	49.37	4.19	99.24	0.35	0.46	14.8	14.48	57.76	18.18	14.6	1.36
12	60.84	61.09	0.75	8.36	11.67	7.31	81.45	0.41	0.39	8.09	8.73	61.98	12.81	9.03	1.03
13	57.36	56.39	0.97	13.13	15.21	4.29	58.13	0.35	0.48	13.07	14.02	57.66	11.44	10.60	1.13
14	52.95	51.28	0.67	16.06	31.78	3.19	76.54	0.46	0.39	18.48	16.68	52.13	14.9	7.25	1.58
15	61.38	60.98	0.4	8.33	33.71	7.32	151.45	0.34	0.48	8.89	8.92	61.46	23.12	16.93	1.88
16	62.88	62.35	0.53	6.4	36.65	9.74	118.64	0.32	0.5	6.7	7.03	63	22.15	16.88	1.36
Min.	51.95	51.28	0.3	6.4	11.3	3.19	30.29	0.31	0.38	6.7	7.03	52.13	11.17	7.25	0.46
Max.	62.88	62.35	1.76	16.13	49.4	9.74	189.27	0.46	0.54	18.48	17.24	63	26.5	18.55	2.12
Av.	**58.64**	**58.01**	**0.63**	**11.78**	**32.96**	**5.35**	**110.28**	**0.35**	**0.46**	**12.56**	**12.49**	**58.85**	**18.89**	**14.06**	**1.35**

Table 4 REE distribution in monazites from dune sediments between Bhavanapadu and Baruva

Grain No.	∑REE	∑LREE	∑HREE	Th+U (Actinoides)	Th/U	∑LREE/Th+U	∑LREE/HREE	Nd/Ce	La/Ce	Th+si	Th+Ca	REE+Y	(∑LLn/HLn)cn	(La/Sm)cn	Eu/Eu*
1	60.40	59.06	0.34	10.78	39.46	5.48	172.71	0.34	0.45	11.39	11.68	59.48	24.37	17.73	2.04
2	60.51	58.58	0.90	8.95	15.27	5.66	64.06	0.36	0.49	8.93	9.52	61.77	11.86	11.14	0.80
3	59.88	57.17	1.71	10.70	30.47	5.34	34.43	0.38	0.45	10.96	11.76	58.80	10.21	9.21	0.94
4	55.12	55.02	1.10	16.94	10.58	4.19	49.11	0.31	0.54	17.91	15.88	55.57	11.05	14.37	1.22
5	60.05	59.44	0.61	10.07	33.72	5.90	97.44	0.29	0.53	10.65	10.92	60.21	16.12	16.78	1.70

6	55.16	54.40	0.76	15.96	31.57	3.41	71.58	0.36	0.44	15.88	16.91	55.48	16.43	12.40	1.32
7	54.05	52.64	0.41	17.74	51.18	3.97	128.39	0.40	0.44	19.47	18.71	53.16	20.02	12.65	1.51
8	57.89	56.39	0.50	9.65	19.53	5.05	115.78	0.41	0.47	9.57	10.64	59.00	18.31	12.80	1.56
9	56.35	55.31	1.04	14.37	45.35	3.85	54.18	0.32	0.42	16.63	14.45	56.83	12.50	10.03	1.42
10	56.26	54.89	2.37	12.86	38.19	4.19	22.74	0.35	0.44	14.55	13.95	57.72	7.60	8.35	0.91
11	57.37	54.92	2.45	13.82	26.64	3.97	22.42	0.41	0.42	14.84	14.47	58.96	8.45	8.31	0.85
12	57.07	54.33	2.74	14.74	9.63	3.69	19.83	0.34	0.48	15.18	13.95	58.86	7.70	9.93	0.85
13	53.33	52.35	1.98	17.98	8.17	2.71	25.93	0.37	0.41	19.33	17.73	54.40	7.64	7.56	0.84
14	62.21	62.80	0.41	9.32	24.21	7.55	153.17	0.34	0.45	9.10	8.41	63.29	26.69	15.32	1.80
15	61.95	60.96	0.99	7.32	21.88	8.33	61.58	0.35	0.46	7.30	8.16	62.28	11.98	10.64	1.44
16	58.21	56.34	0.87	13.82	23.25	4.08	64.76	0.39	0.45	14.78	14.48	57.41	12.65	8.69	0.92
Min.	53.05	51.35	0.34	7.32	8.17	2.71	19.83	0.29	0.41	7.30	8.16	53.16	7.60	7.56	0.77
Max.	63.21	62.80	2.74	18.98	51.18	8.33	173.71	0.41	0.54	19.47	18.71	63.29	26.69	17.78	2.04
Av.	**57.94**	**56.75**	**1.20**	**12.57**	**26.46**	**4.96**	**71.25**	**0.36**	**0.46**	**13.25**	**13.00**	**58.52**	**13.80**	**11.45**	**1.23**

Fig.1 Map of the study area and sample locations.

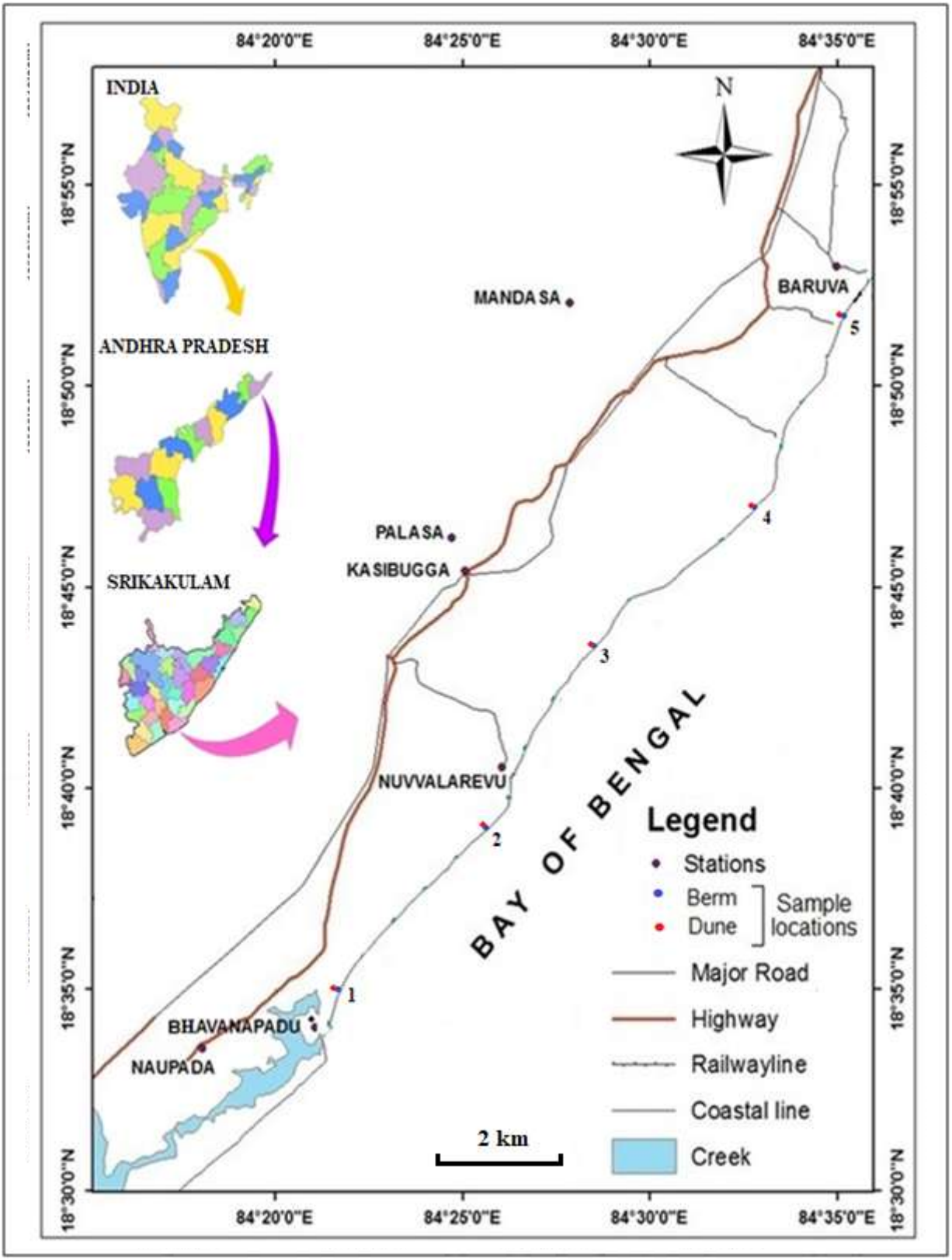

Fig.2 Geological map of the study area (Source: Geological Survery of India).

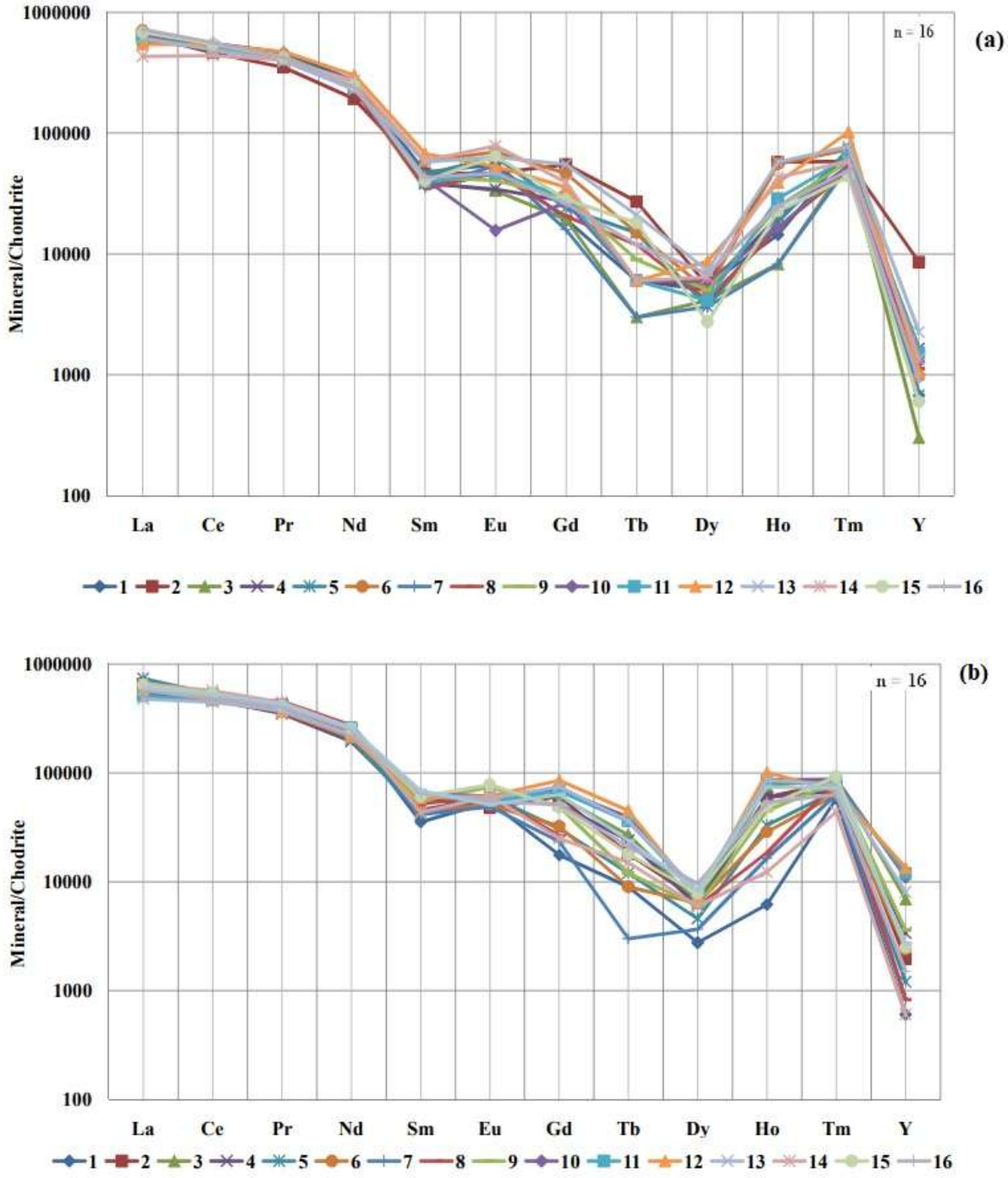

Fig. 3 Chondrite normalized plot showing the rare earth elements distribution inselected monazites from (a) Berm and (b) Dune sediments of study area (Taylor and Mc Lennon, 1985)